Spontaneous Periodic Diameter Oscillations in InP Nanowires: The Role of Interface Instabilities

ARTICLE *in* NANO LETTERS · DECEMBER 2012

Impact Factor: 13.59 · DOI: 10.1021/nl302891b · Source: PubMed

4 AUTHORS:

Douglas Oliveira
University of Campinas
7 PUBLICATIONS **30** CITATIONS
SEE PROFILE

Luiz H G Tizei
French National Centre for Scientific Research
30 PUBLICATIONS **153** CITATIONS
SEE PROFILE

Daniel Ugarte
University of Campinas
135 PUBLICATIONS **9,441** CITATIONS
SEE PROFILE

Mônica A Cotta
University of Campinas
127 PUBLICATIONS **989** CITATIONS
SEE PROFILE

NANO LETTERS

Letter

pubs.acs.org/NanoLett

Spontaneous Periodic Diameter Oscillations in InP Nanowires: The Role of Interface Instabilities

D. S. Oliveira,* L. H. G. Tizei,† D. Ugarte, and M. A. Cotta

Instituto de Física "Gleb Wataghin", Universidade Estadual de Campinas, UNICAMP, 13083-859, Campinas, SP, Brazil

Supporting Information

ABSTRACT: We have observed that thin InP nanowires generated by vapor−liquid−solid growth display spontaneous periodic diameter oscillations when large group III supersaturations are used. Diameter variations are associated with a large number of stacking faults and crystallographic phase changes(wurtzite/zinc-blende); also the axial distance between oscillations depends on the indium precursor flow used during the run. We attribute the morphology changes to a substantial deformation of the triple phase line (vapor−liquid−solid) at the catalyst nanoparticle edge originated from multistep nucleation during growth. The deformation alters the mechanical force balance acting on the nanoparticle during growth in such a way that the particle displaces from the nanowire top and wets the nanowire sidewall. Subsequently, as catalytic growth occurs at the sidewall, the associated increase in diameter will eventually push the NP back to its original wire-top position until the onset of a new instability at the triple phase line.

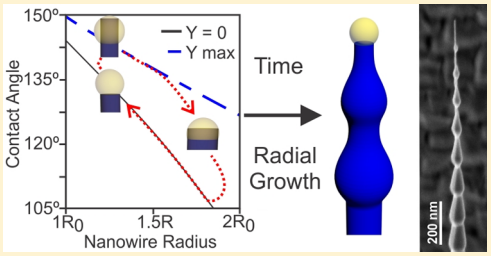

KEYWORDS: *Nanowire, InP, vapor−liquid−solid, wetting, kinetic roughness*

Semiconductor nanowires (NWs) show promising applications for new generations of devices due to their electronic properties and geometric configurations. Among materials currently exploited to fabricate NWs, III−V compounds show interesting characteristics in terms of band gap and surface properties.[1−5] However, we must yet obtain a full control of crystal structure and morphologies in order to develop such applications.

Under specific growth conditions, III−V nanowires grown by the vapor−liquid−solid[6] (VLS) method can easily exhibit a wurtzite (WZ) phase that is not observed in thin films of the same semiconductor material. The possibility of growing different crystallographic phases of the same material allowed achieving twinned superlattices or heterostructures of a single composition.[7−9] Recent reports have shown that the crystal structure influences drastically the electric properties of InP nanowires; zinc blende (ZB) segments behave as quantum wells orthogonal to current path in WZ nanowires.[10] Moreover, a mixture of ZB and WZ segments in InAs NWs can exhibit up to 2 orders of magnitude higher resistivity than single-phase NWs; in contrast, stacking faults and other defects do not show significant effects on the InAs nanowire resistivity.[11] From another point of view, NW morphology is also affected by phase changes and the corresponding facet orientations[8] or by diameter variations due to the presence of a large number of stacking faults.[12] These morphology changes have inspired new fields of applications such as thermoelectric devices[13] or as highly absorbing media for solar cells.[14]

Despite the huge advance in control of both NW morphology[15] and crystal structure,[16,17] many questions about such issues in VLS growth remain unclear, particularly on the behavior of the triple-phase-line (TPL). Glas et al.[18] have shown that TPL formation energies for a WZ and a ZB nuclei explains the preferential growth of WZ or ZB GaAs nanowires depending on the catalyst supersaturation. Oh et al.[19] used in situ measurements to reveal that TPL presents an oscillatory behavior during growth, which was attributed to the saturation of the catalyst particle before nucleus formation. In addition, Tizei et al.[20] have shown that the VLS growth of InP nanowires is accelerated by the presence of a screw dislocation, which may also impact on the TPL behavior.

It is interesting to note that quite a different nanoparticle (NP) equilibrium position during VLS growth has been proposed by Dubrovskii et al.[21] to explain the growth of ZB GaAs NWs catalyzed by Ga droplets. In their model, the NP wets the sidewalls and surrounds the NWs instead of resting on top of the NW when growth is carried out with a lower surface energy metal. Along the same line of ideas, contact angles and surface energies are altered with the introduction of dopants during InP growth[7] or by a geometrical deformation of the TPL that has been related to the formation of stacking faults (SFs) in WZ InP NWs.[12] In the latter case, the authors considered that the TPL deformation is associated with kinetic roughening of the metal−semiconductor interface due to excess In supplied during growth. The In atoms are simultaneously incorporated through the NP as well as directly at TPL; the multistep nucleation resulting from the competition between these two processes can lead to stacking faults as a path to reach a local

Received: August 3, 2012
Revised: October 30, 2012
Published: December 3, 2012

   dx.doi.org/10.1021/nl302891b | *Nano Lett.* 2013, 13, 9−13

minima of system interface and surface energy. This interpretation also predicts that the probability of SF formation will depend on NP size because larger sizes allow a larger number of nucleating sites along the TPL and thus larger instabilities and defect densities, as experimentally observed. However, in that work the geometry of the NWs presenting larger densities of SFs also show diameter variations along the NW length while the pure WZ InP NWs present a conical, tapered shape.

Here, we investigate the geometry of InP NWs grown with small (5 and 20 nm diameter) gold NPs under large In precursor flows. These nanowires display periodic diameter modulations along the axial direction (Figure 1), even though

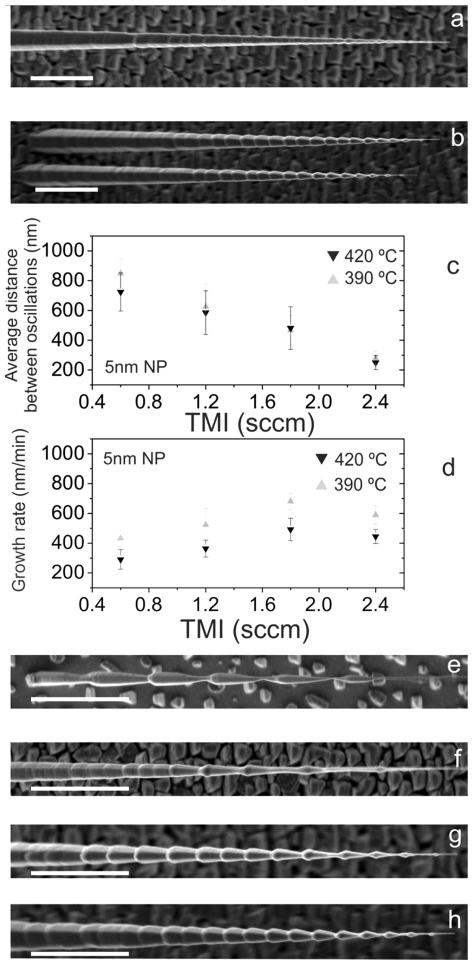

Figure 1. (a,b) SEM images of InP nanowires grown at 390 °C with diameter of NPs ~20 nm (a) and ~5 nm (b). (c,d) Average distance between diameter oscillations along InP NW and growth rate as a function of TMI flow during the run, respectively, for NWs grown with ~5 nm NPs (values in the plots obtained from projected lengths in SEM images). (e–h) Typical morphologies of InP nanowires grown at 390 °C under 0.6, 1.2, 1.8, 2.4 sccm TMI flows, respectively and NP diameter ~5 nm. Scale bar, 1 μm.

growth conditions have been kept constant throughout the run. The diameter modulations increase in periodicity with the TMI flow. This oscillatory diameter behavior correlates with phase changes; larger diameters are mostly ZB instead of the dominant WZ structure usually observed for InP NWs and at the thinner regions of our samples. We attribute our NW morphology to a growth model that periodically alternates between the sidewall wetting VLS[21] and standard VLS models.[6] Thus, our analysis introduces new elements in the growth dynamics that can contribute to NW crystal phase and morphology control.

InP NWs were grown on GaAs(100) substrates in a chemical beam epitaxy (CBE) chamber, using colloidal Au NPs as the catalyst material. The substrate native oxide was not desorbed prior to the InP growth. The average diameters of the catalysts were 5 or 20 nm. Trimethylindium (TMI) diluted with hydrogen carrier gas and thermally decomposed phosphine (PH3) were used as group III and V sources, respectively. PH3 flow (at 10 sccm) and growth time were kept constant throughout the run for all samples. TMI flows were varied in the range from 0.6 to 2.4 sccm from run to run. Our samples were analyzed by scanning electron microscopy (SEM, Zeiss Supra 55) for statistical information about geometry, morphology, and composition, using energy dispersive X-ray spectroscopy (EDS) (SEM, FEI Inspect F50). We have also used transmission electron microscopy (TEM, JEM 3010 URP operated at 300 kV and a JEM 2100 ARP operated at 200 kV) for structural analysis.

The range of TMI flow was chosen in order to reproduce and extend the results presented by Chiaramonte et al;[12] for the NWs grown with 20 nm NPs we have observed diameter variations similar to those reported by these authors. However, we were surprised by the fact that the majority (79% of 107 analyzed wires) of the NWs in the samples grown with 5 nm NPs presented a remarkable periodic diameter modulation that was unexpected for the constant growth conditions used during the whole run. Also, the periodicity of diameter modulation along the NW is more uniform for NWs grown with smaller (5 nm) NPs (see Figure 1a,b); however, at the base of the NWs (closer to the substrate), the diameter oscillations are not so clearly visible as near the apex. This may be due to vapor–solid (VS) growth at the NW sidewall, since mass transport from the substrate surface to the base of the NWs has been discussed by many authors in literature[22–24] as the source of the conical or tapered NW shapes at lower temperatures. Changing the substrate from GaAs to InP enhances polycrystal film deposition on the substrate surface and minimizes mass transfer to NW sidewall. Indeed, the shape of the NWs grown on InP substrates is less tapered, and the diameter oscillations are clearly visible from base to apex, as well as the enhanced polycrystal deposition on the surface (Figure S1 in Supporting Information).

The average axial distance between subsequent diameter maxima, as well as the growth rate of the NWs (Figure 1c–g), were measured from SEM images for NWs presenting the same spatial orientation along the [111] direction of the GaAs substrate. Figure 1c shows that, for NWs grown with 5 nm NPs, the distance between diameter oscillations diminishes as the TMI flow increases; moreover, the growth rate is not linear with this parameter (Figure 1d). We must keep in mind that the TMI flow values used here are larger than those reported by Chiaramonte et al.,[12] who has previously proposed the hypothesis of competition between different routes of In incorporation. These authors considered that In incorporation through the NP could be limited either due to the low TMI pyrolysis rate leading eventually to a surface saturation with methyl radicals[25] or due to smaller V/III ratios as TMI flow is increased what induces low availability of phosphorus atoms at the NP-NW interface. Our data (Figure 1d) shows slightly smaller growth rates at higher temperatures, suggesting that the

dx.doi.org/10.1021/nl302891b | Nano Lett. 2013, 13, 9–13

latter scenario is more likely to occur. In fact, higher temperatures can lower the growth rate due to the re-evaporation of P_2 from the growing surface. This effect should overcome the increase of P diffusion length at higher temperatures, which could scale up the supply of P atoms at the metal−semiconductor interface. On the other hand, TMI pyrolysis and methyl radical desorption would be favored as temperature rises; the growth rate should increase with temperature until desorption of partly cracked species takes place.[26]

It is important to emphasize that our nanowires have a small NP/NW interface area when compared with most reports in literature.[7,12,27,28] In addition, our nanowire growth rates (>300 nm/min, or >15 monolayers/s) imply very short catalyst saturation, nucleation and monolayer formation times. Therefore, events that can occur while the nucleus is propagating in order to complete a monolayer (a process experimentally observed to take about 0.1 s[19]) must be considered as well, such as simultaneous nucleation of several monolayers and the consequent TPL deformation.[12] From the energetic point of view, a rough metal−semiconductor interface due to the simultaneous nucleation of several monolayers should show a free energy increase depending on step density.[29] The balance of surface energies determines the contact angle of the NP and consequently the forces acting on it. Thus, in order to dynamically minimize the interface energy, a local increase in contact angle may occur. Figure 2a schematically shows the normal forces on the NP when the TPL is randomly shifted downward.[21] Under normal VLS conditions, with $\theta > \pi/2$ and a fast response of the liquid compared to the growth rate of the solid the normal force should be directed upward in order to restore the equilibrium position of the NP on top of the NW provided that[30]

$$\gamma_{LV} \sin\theta + \gamma_{SL} - \gamma_{SV} \cos\phi > 0 \quad (1)$$

where γ_{SV}, γ_{SL}, and γ_{LV} are the surface energies of the lateral of the nanowire and vapor interface, the lateral−liquid interface and the liquid−vapor interface respectively, θ is the contact angle of the nanoparticle, and ϕ is the angle between the nanowire sidewall and its growth axis.

In our case, this angle should vary along the NW during growth; at regions of maximum diameter along the nanowire, ϕ is about 10° (see Figure S2 in Supporting Information) and cos ϕ ~1. However, at the very large supersaturations and growth rates employed here, we can expect large enough deformations of the TPL that the liquid can only accommodate by locally varying the contact angle. Therefore, if the deformation at the TPL triggers a sufficiently large increase in the contact angle θ, the NP position would become unstable. In such scenario, depending on the magnitude of the contact angle, the NP experiences a downward force and starts to wet the sidewall of the NW.

However, this sidewall wetting process continuously changes the position of the TPL; the NW may now grow laterally due to the new TPL position despite the different surface energies involved, since the NP acts as a material reservoir. If this process continues, eventually a whole lateral section of the NW will be wet by the NP. This scenario agrees with our SEM images of the diameter-modulated NWs which show an asymmetry of the enlarged sections with regard to the NW axis (Figure S3 in Supporting Information).

As the NP wets the sidewall in a larger extent with height Y, we can again consider the NP as spherically symmetric and calculate the relation between contact angle and NW radius, as a function of the height Y (Figure 2a). For these calculations, we have considered a constant volume of the NP as the only constraint in the system. This hypothesis is supported by EDS measurements in our NWs which have shown similar In/Au ratios (within the resolution of this technique) at the NP.

First, we will consider a small increase in the NW radius while Y increases; looking at Figure 2 we can notice that the contact angle increases with Y, so the NP must be pushed downward even further. As pointed out by Dubrovskii et al.,[31] eq 1 is basically the same condition for nucleation at the TPL under equilibrium conditions as discussed by Glas et al.[18] In that case, the wurtzite phase is favored at high liquid supersaturations. Thus, for nucleation on top of the NW while the TPL is pushed downward, we may expect a crystallographic phase change from WZ to ZB as the NW radius starts to grow. This behavior can be indeed observed in high-resolution TEM images (HRTEM) of the region with diameter variation (Figure 2b). We can identify a very large density of SFs as the NW diameter begins to grow; also phase changes, from WZ to ZB, occur in these larger diameter areas. Our measurements along the whole length of three different NWs show that the small diameter regions are (83 ± 8)% WZ, while the large diameter regions are (80 ± 10)% ZB with a large number of twins. Thus the NW enlarged region shows ZB as the dominant phase.

A model for VLS growth with the NP wetting the NW sidewall along a height Y has been recently proposed by Dubrovskii et al.[21] The authors calculated a stable NP position at the maximum Y value (Y_{max}) which corresponds to the point where the top of the semiconductor cylinder reaches the NP

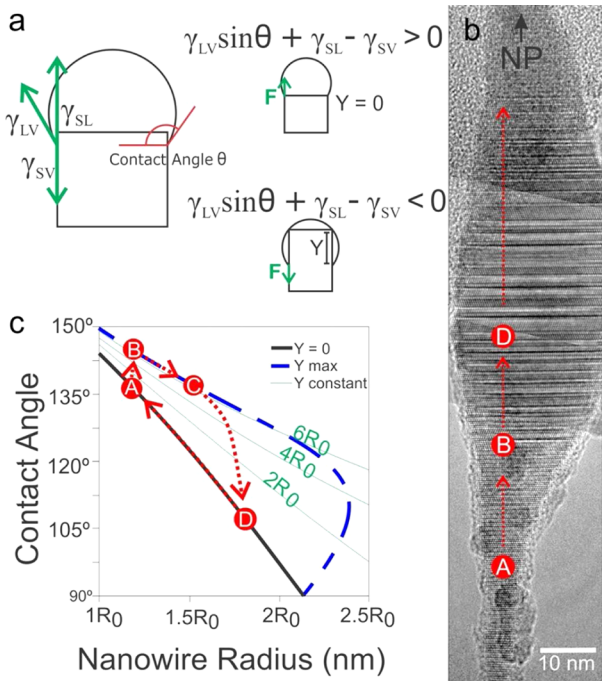

Figure 2. (a) Diagram of surface energies and contact angle concerning the stability of the catalyst on top of the nanowire. (b) HRTEM image of a diameter oscillation of a typical InP NW grown at 390 °C under 2.4 sccm TMI flow with ~5 nm NP. The red dots make reference to the graph on (c), which shows the contact angle dependence on nanowire radius for a catalyst with constant volume, as a function of the wet sidewall height, Y.

dx.doi.org/10.1021/nl302891b | Nano Lett. 2013, 13, 9−13

surface. In that model, however, the authors considered the NW radius constant throughout the process, despite a slight increase in diameter along NW length for Ga-catalyzed GaAs NWs.[21,32] If we now consider the NP at Y_{max}, for any increase in the NW diameter to occur, we expect a corresponding decrease in the contact angle. Equation 2 shows the geometrical relationship for a spherical cap representing the NP[21] in terms of contact angle θ, NP volume V, radius of the spherical cap (assumed equal to the nanowire radius) R, and the lateral height Y:

$$V = \frac{\pi R^3}{3}\frac{(1-\cos\theta)^2(2+\cos\theta)}{\sin^3\theta} - \pi R^2 Y \quad (2)$$

If we consider a constant NP volume V and height Y, we can plot (Figure 2c) the relationship between R and θ according to eq 2. Y_{max} relates with these variables by

$$Y_{max} = 2R\tan(\theta - 90^\circ) \quad (3)$$

Figure 2c shows that changes in contact angle can accommodate an increase up to a factor 2 in the NW radius.

We will now consider a different situation where the instability created by roughening at the liquid−solid interface for the NP on top of the NW ($Y = 0$) can locally increase the contact angle while keeping the radius essentially constant. The downward force on the NP causes it to wet the NW sidewall up to an extension Y (A to B in Figure 2c); the TPL deformation is thus enhanced and catalyzed lateral growth would lead to a larger NW radius. However, as the radius increases, the contact angle decreases and the force on the NP eventually changes from downward to upward (C in Figure 2c), depending on the magnitudes of surface energies involved, according to eq 1. This upward force pushes the NP back toward the top of the NW ($Y = 0$), and the radius slowly starts to shrink. Moreover, the increase in NW radius can also lead to a temporarily smaller axial growth rate which allows the TPL to recover its equilibrium shape. Moreover, the position of the TPL during this process determines the dominant crystallographic phase in each region along the NW, as indicated by the dots in Figure 2b. Furthermore, since the origin of the instability is related to the In flow and to the interface area, we can expect roughness to build up again as growth proceeds, thus creating an oscillatory process.

On the other hand, for a larger NP, simultaneous multistep nucleation can take place at a larger number of sites along the TPL; moreover, the step propagation time along the NP/NW interface is also longer due to the larger area. Thus, a wider spectrum of spatial frequencies and smaller amplitudes for TPL deformation can be expected for larger NPs. In this case, diameter variations as well as phase changes will be random and periodicity more difficult to be achieved. We experimentally notice that samples grown with larger NPs (20 nm) under the same conditions show a larger dispersion in morphology with diameter oscillations present in only a small fraction of the NWs (Figure S4 in Supporting Information). Furthermore, periodic oscillations should not be observed for nanowires with initial contact angle below a certain value (estimated as 120°); instead, the NP could be torn apart or slide down along the entire NW. Indeed, we observe lateral branches on sidewalls and even changes of the NW axial direction for NWs grown with larger NPs, as shown in Figure 3.

Morphologies such as those shown in Figure 3 are seldom observed for the 5 nm NWs. In the latter case, diameter

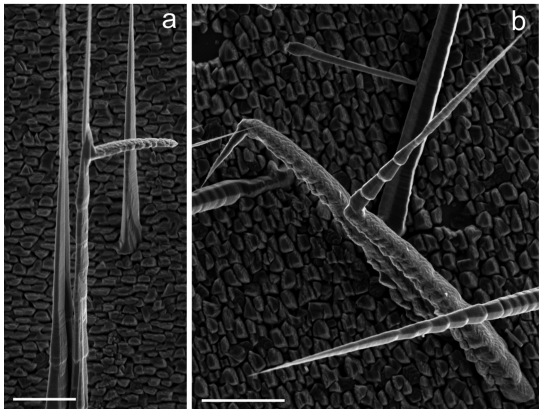

Figure 3. SEM images of InP NWs grown using ~20 nm diameter gold NPs as catalyst and TMI flow 2.4 sccm at (a) 390 °C and (b) 420 °C. Scale bar, 1 μm.

enlargement (and the subsequent gradual return to the original diameter) allows the NP to reach a more stable position on top of the NW.[21] The NP will continue at this position with random forces acting upon it until a new, large geometrical deformation of the TPL changes the stability of the NP again. This process depends strongly on the impingement rate of In atoms on the surface. Thus, a larger number of oscillations and a smaller average distance between them is expected when larger TMI flows are used. Furthermore, major changes in position of the NP during growth determine the dominant phase (WZ or ZB) in each corresponding region along the NW depending on the dominant nucleation site in each case. Our interpretation is also supported by recent work[33] that points to small TPL spatial shifts as the origin of dominant crystal structure and defect formation during growth of self-catalyzed GaAs nanowires. The TPL shift is controlled by growth parameters such as precursor flows; using this mechanism as a guideline, the authors successfully demonstrated controllable fabrication of two distinct types of axial superlattice GaAs NWs consisting of zinc-blende/defect-section and wurtzite/defect-section units.

In conclusion, we have observed the formation of WZ InP nanowires with spontaneously formed periodic diameter oscillations; the regions with larger diameter are associated with a large number of SFs with the eventual transition in the dominant crystallographic phase (from WZ to ZB). The distance between the oscillations strongly depends on the Indium precursor flow. These morphologies were obtained using constant parameters during growth and in our interpretation are associated with growth instabilities which cause a periodic transition between the traditional VLS growth model[6] and the lateral wetting VLS model proposed by Dubrovskii et al.[21] We also propose that the driving force for this transition originates at the TPL deformation due to competition between the routes of In incorporation during growth. Catalytic radial growth allows a transient drop in axial growth rate through diameter enlargement. The formation of SFs and crystallographic phase changes occur due to the deformation of the TPL and the balance of mechanical forces acting on the NP (pushing it upward or downward), which is periodically altered during growth. Our results thus suggest a new growth dynamics of InP NWs that can be exploited to create new heterostructures of a single material.

dx.doi.org/10.1021/nl302891b | *Nano Lett.* 2013, 13, 9−13

■ ASSOCIATED CONTENT

Supporting Information

Additional figures. This material is available free of charge via the Internet at http://pubs.acs.org.

■ AUTHOR INFORMATION

Present Address

[†]Laboratoire de Physique des Solides, Université Paris-Sud, CNRS-UMR 8502, Orsay 91405, France.

Notes

The authors declare no competing financial interest.

■ ACKNOWLEDGMENTS

The authors thank the Laboratory of Electron Microscopy at the National Laboratory of Nanotechnology (LNNANO/CNPEM) for granting access to the electron microscopy instruments used in this work. We also acknowledge Th. Chiaramonte for discussions on NW growth and H. T. Obata for technical assistance. This work was supported by FAPESP, CNPq, and CAPES.

■ REFERENCES

(1) Yan, R.; Gargas, D.; Yang, P. *Nat. Photonics* **2009**, *3*, 569−576.
(2) Duan, X.; Huang, Y.; Cui, Y.; Wang, J.; Lieber, C. M. *Nature* **2001**, *409*, 66−9.
(3) Moreau, A. L. D.; Janissen, R.; Santos, C. a.; Peroni, L. a.; Stach-Machado, D. R.; de Souza, A. A.; de Souza, A. P.; Cotta, M. A. *Biosen. Bioelectron.* **2012**, *36*, 62−68.
(4) Mokkapati, S.; Jagadish, C. *Mater. Today* **2009**, *12*, 22−32.
(5) Chau, R.; Doyle, B.; Datta, S.; Kavalieros, J.; Zhang, K. *Nat. Mater.* **2007**, *6*, 810−2.
(6) Wagner, R.; Ellis, W. *Appl. Phys. Lett.* **1964**, *4*, 89−90.
(7) Wallentin, J.; Ek, M.; Wallenberg, L. R.; Samuelson, L.; Deppert, K.; Borgström, M. T. *Nano Lett.* **2010**, 4807−4812.
(8) Caroff, P.; Dick, K.; Johansson, J.; Messing, M.; Deppert, K.; Samuelson, L. *Nat. Nanotechnol.* **2008**, *4*, 50−55.
(9) Algra, R. E.; Verheijen, M. A; Borgström, M. T.; Feiner, L.-F.; Immink, G.; van Enckevort, W. J. P.; Vlieg, E.; Bakkers, E. P. A. M. *Nature* **2008**, *456*, 369−72.
(10) Wallentin, J.; Ek, M.; Wallenberg, L. R.; Samuelson, L.; Borgström, M. T. *Nano Lett.* **2012**, *12*, 151−5.
(11) Thelander, C.; Caroff, P.; Plissard, S.; Dey, A. W.; Dick, K. a *Nano Lett.* **2011**, *11*, 2424−9.
(12) Chiaramonte, T.; Tizei, L. H. G.; Ugarte, D.; Cotta, M. A. *Nano Lett.* **2011**, *11*, 1934−1940.
(13) Zianni, X. *Appl. Phys. Lett.* **2010**, *97*, 233106.
(14) Diedenhofen, S. L.; Janssen, O. T. A; Grzela, G.; Bakkers, E. P. A. M.; Gómez Rivas, J. *ACS Nano* **2011**, *5*, 2316−23.
(15) Plissard, S. R.; Slapak, D. R.; Verheijen, M. A.; Hocevar, M.; Immink, G. W. G.; Weperen, I.; van; Nadj-Perge, S.; Frolov, S. M.; Kouwenhoven, L. P.; Bakkers, E. P. A. M. *Nano Lett.* **2012**, *12*, 1794−8.
(16) Ross, F. M. *Rep. Prog. Phys.* **2010**, *73*, 114501.
(17) Joyce, H. J.; Wong-Leung, J.; Gao, Q.; Tan, H. H.; Jagadish, C. *Nano Lett.* **2010**, *10*, 908−15.
(18) Glas, F.; Harmand, J.-C.; Patriarche, G. *Phys. Rev. Lett.* **2007**, *99*, 3−6.
(19) Oh, S. H.; Chisholm, M. F.; Kauffmann, Y.; Kaplan, W. D.; Luo, W.; Rühle, M.; Scheu, C. *Science (New York)* **2010**, *330*, 489−93.
(20) Tizei, L. H. G.; Craven, A. J.; Zagonel, L.; Tencé, M.; Stéphan, O.; Chiaramonte, T.; Cotta, M. A.; Ugarte, D. *Phys. Rev. Lett.* **2011**, *107*, 1−5.
(21) Dubrovskii, V. G.; Cirlin, G. E.; Sibirev, N. V.; Jabeen, F.; Harmand, J. C.; Werner, P. *Nano Lett.* **2011**, *11*, 1247−53.
(22) Dayeh, S. A.; Yu, E. T.; Wang, D. *Nano Lett.* **2009**, *9*, 1967−72.
(23) Plante, M. C.; LaPierre, R. R. *J. Appl. Phys.* **2009**, *105*, 114304.
(24) Mohammad, S. N. *Nano Lett.* **2008**, *8*, 1532−8.
(25) Kobayashi, Y.; Kobayashi, N. *Jpn. J. Appl. Phys.* **1992**, *31*, L71.
(26) Kobayashi, N.; Benchimol, J. L.; Alexandre, F.; Gao, Y. *Appl. Phys. Lett.* **1987**, *51*, 1907.
(27) Paiman, S.; Gao, Q.; Tan, H. H.; Jagadish, C.; Pemasiri, K.; Montazeri, M.; Jackson, H. E.; Smith, L. M.; Yarrison-Rice, J. M.; Zhang, X.; Zou, J. *Nanotechnology* **2009**, *20*, 225606.
(28) Watanabe, Y.; Hibino, H.; Bhunia, S.; Tateno, K.; Sekiguchi, T. *Phys. E* **2004**, *24*, 133−137.
(29) Tsao, J. Y. *Materials Fundamentals of Molecular Beam Epitaxy*, 1st ed.; Academic Press: New York, 1992; p 301.
(30) Nebol'sin, V.; Shchetinin, A. *Inorg. Mater.* **2003**, *39*, 899−903.
(31) Dubrovskii, V. G. *Tech. Phys. Lett.* **2011**, *37*, 53−57.
(32) Rudolph, D.; Hertenberger, S.; Bolte, S.; Paosangthong, W.; Spirkoska, D.; Döblinger, M.; Bichler, M.; Finley, J. J.; Abstreiter, G.; Koblmüller, G. *Nano Lett.* **2011**, *11*, 3848−54.
(33) Yu, X.; Wang, H.; Lu, J.; Zhao, J.; Misuraca, J.; Xiong, P.; von Molnár, S. *Nano Lett.* **2012**, *12*, 5436−5442.